Oxygen carrier development of calcium manganite-based materials with perovskite structure for chemical looping combustion of methane

Patrick Moldenhauer[1,*], Peter Hallberg[1], Max Biermann[1],
Frans Snijkers[2], Knuth Albertsen[3], Tobias Mattisson[1], Anders Lyngfelt[1]

[1] Chalmers University of Technology, Department of Energy and Environment, 412 96 Gothenburg, Sweden
[2] Flemish Institute for Technological Research NV (VITO), Unit Sustainable Materials Management, 2400 Mol, Belgium
[3] Euro Support Advanced Materials B.V., 5405 AH Uden, The Netherlands
* Corresponding author (patrick.moldenhauer@chalmers.se)

Abstract – Chemical-looping combustion (CLC) of gaseous fuels could be of interest in industrial processes for heat, power or hydrogen production with carbon capture. For instance, production of steam or hydrogen from refinery gas are possible applications. A series of collaborate European projects has been carried out since 2002, which focused on oxygen-carrier development and upscaling of both the CLC process and oxygen-carrier production with methane or natural gas as fuel. Most recently, in the FP7 SUCCESS project (2013-2017), Ca-Mn-based materials with perovskite structure, $CaMnO_3$, were produced at a larger scale and with cheap and commercial raw materials. The main advantage with this type of oxygen carrier is the ability to release oxygen to the gas phase, hence promoting reactivity in the fuel reactor. In the project, a significant number of such materials were produced and tested. It was found that a perovskite structure can be obtained relatively easy with widely different raw materials for Ca, Mn, Ti and Mg. The produced materials generally had high reactivities and high attrition resistances, but were prone to sulfur poisoning.

In this paper, selected results are presented from the different stages of material development and upscaling, i.e., from bench-scale reactors with batch and continuous operation, respectively, as well as from a laboratory-scale unit with continuous operation and a nominal fuel input of 10 kW_{th}. In the 10 kW unit, the gas velocities in the riser and in the grid jet zone of the gas distributor come close to gas velocities of industrial-scale units and, therefore, this unit is used to assess particle lifetime. Results from the 10 kW unit show that very high degrees of fuel conversion can be reached while achieving very high lifetimes.

1 INTRODUCTION

1.1 Chemical-Looping Combustion

Chemical-looping combustion (CLC) is an innovative method to oxidize fuels with inherent sequestration of CO_2. The most common adaptation of CLC is based on two interconnected, chemical reactors: In the air reactor (AR) air is used to oxidize a solid oxygen-carrier, and in the fuel reactor (FR) fuel is added and oxidized by the oxygen carrier, which, in turn, is reduced. In this way the combustion products are not diluted with nitrogen and, after condensation of steam, the fuel-reactor flue gas ideally

consists of pure CO_2. In contrast to other carbon capture technologies, such as absorption or adsorption of CO_2 or oxyfuel combustion, there is no direct energy penalty for gas separation associated with chemical-looping combustion. General information about chemical-looping as well as an overview of trends and developments can be found elsewhere [1, 2].

Suitable process temperatures vary slightly for different oxygen-carrier materials, but are usually considered to be within the range of 800-1050°C. The most commonly proposed way to design a chemical-looping combustor is to use circulating fluidized-beds (CFBs) with oxygen-carrier particles as bed material instead of an inert bed material used in conventional applications. Commonly proposed oxygen carrier materials include transition metal oxides such as NiO, Fe_2O_3, CuO or Mn_3O_4, with or without inert support materials such as, for example, Al_2O_3 or ZrO_2 [3].

In regular chemical-looping combustion, a gaseous fuel is assumes to react with the solid oxygen carrier. However, some oxygen-carrier materials can release gaseous oxygen, which was found to enhance fuel conversion. This process is referred to as chemical-looping with oxygen uncoupling (CLOU) [4].

1.2   Oxygen Carrier Development in EU-financed, collaborative projects

In Europe, the CLC technology for gas using circulating fluidized-beds has to a large extent been developed through a series of EU-financed collaborative projects. Initially, in the GRACE project (2002-2003), nickel-based oxygen-carrier materials were identified as highly promising. Materials were developed, which could achieve very high, but incomplete, levels of gas conversion [5]. In the project CLC Gas Power (2006-2008), optimization of Ni-based materials was carried out using spray-drying and impregnation; production methods which are suitable for large scale application. [6]. Thermodynamic limitations of nickel-based materials, which inhibit full conversion of fuel, as well as toxicity issues soon led development away from nickel and towards highly reactive and environmentally benign materials, i.e., materials based on copper, manganese, iron manganese and – the focus of this paper – calcium manganite. The latter has a perovskite structure and CLOU properties, i.e., the particles release gas-phase oxygen in the fuel reactor. A gas–gas reaction of oxygen and fuel, in contrast to a gas–solid reaction in regular CLC, can potentially achieve complete fuel conversion at much lower solids inventories. In the INNOCUOUS project (2010-2013), different materials based on calcium manganite were developed, out of which those doped with Ti and Mg showed the most promising results [3]. In the recently concluded project SUCCESS (2013-2017), the production of one of these materials through spray-drying was scaled up to the multi-tonne scale. This was achieved by using raw-materials that are commercially available as well as adapting the spray-drying and sintering process to suit large-scale production. Figure 1 shows the development route of calcium manganite-based oxygen carriers over the EU-financed projects INNOCUOUS and SUCCESS.
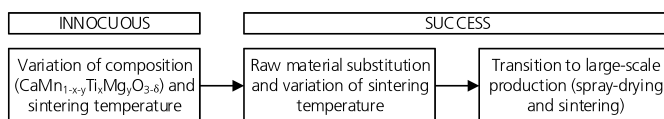

INNOCUOUS	SUCCESS	
Variation of composition (CaMn$_{1-x-y}$Ti$_x$Mg$_y$O$_{3-\delta}$) and sintering temperature	Raw material substitution and variation of sintering temperature	Transition to large-scale production (spray-drying and sintering)

Figure 1: Development route of calcium manganite-based oxygen carriers in different EU-financed projects

1.3 Scope

The focus of this paper is on the experimental testing of different calcium manganite-based oxygen-carrier materials within the SUCCESS project. The experimental units in focus are two laboratory-scale chemical-looping combustion reactors that are operated continuously with respect to fuel feeding and oxygen-carrier circulation. The nominal fuel loads of the reactors are 300 W and 10 kW, respectively. Figure 2 shows detailed development schemes for the tasks raw-material substitution and up-scaling, cf. Figure 1, with the experimental testing in focus highlighted.

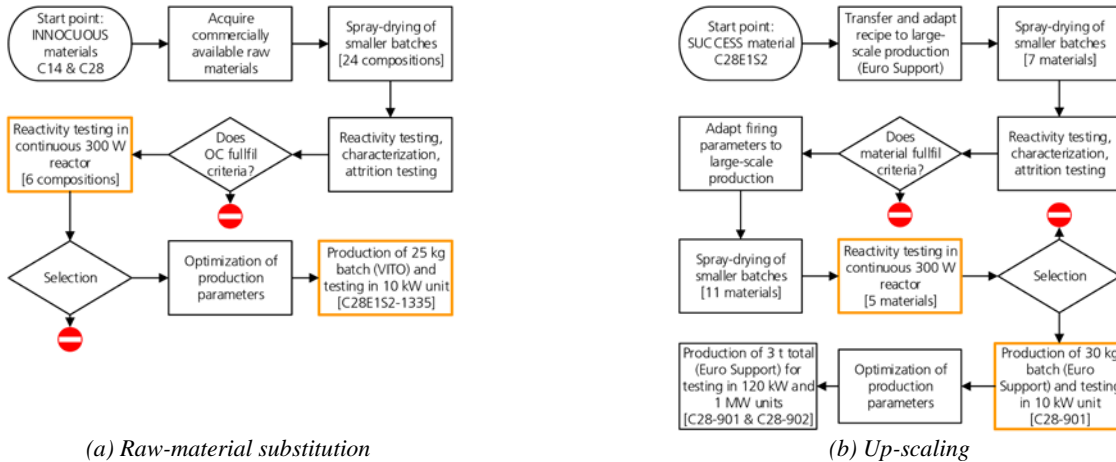*(a) Raw-material substitution*　　　　　　　　　　　*(b) Up-scaling*

Figure 2: Detailed development schemes of calcium manganite-based oxygen carriers in the SUCCESS project for the tasks (a) raw-material substitution and (b) up-scaling.

2 EXPERIMENTAL

2.1 Chemical-Looping Test Units

2.1.1 300 W Unit

The laboratory-scale continuous 300 W unit requires approximately 250-400 g of oxygen-carrier particles, depending on their density. The reactor is 300 mm high and has two reactor chambers: an air reactor fluidized with air and a fuel reactor fluidized with methane. The fuel reactor has a cross-section of 25 mm x 25 mm, whereas the base of the air reactor is 25 mm x 42 mm and contracts to 25 mm x 25 mm in the riser section. Figure 3 shows the working principle of the reactor unit: high gas velocities cause the particles to leave the air reactor and enter the gas-solid separator placed on top flange of reactor unit (not shown). The particles fall back and enter the inlet of the J-type loop seal (downcomer). This causes particles at the outlet of the loop seal to drop down onto the bubbling bed of the fuel reactor (through the return orifice). From the bottom of the fuel reactor the particles flow back into the air reactor via the lower loop-seal. The air reactor is fluidized with air, the loop seals are fluidized with argon and the fuel reactor is fluidized with either methane (fuel operation) or argon (determination of CLOU behavior).
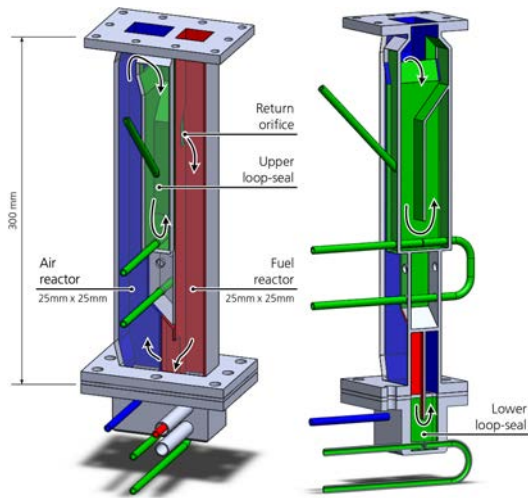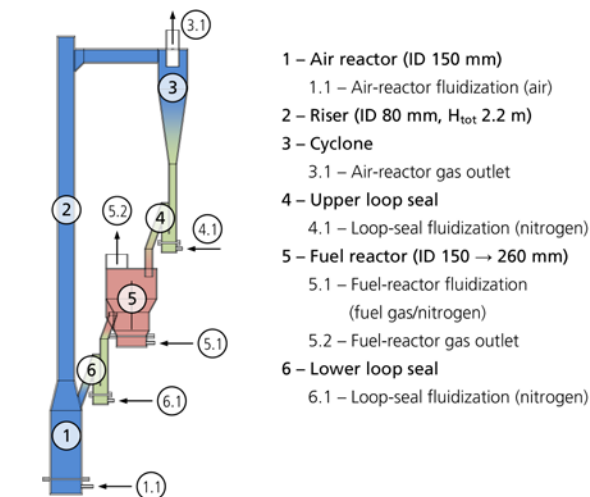
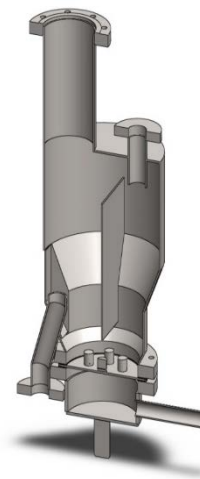*Figure 3: Illustration of the 300 W chemical-looping combustion reactor*

The off-gases from the reactors are separately cooled to 4°C and filtered. The fuel-reactor flue gas passes a water seal, which generates a slight over pressure in the fuel reactor and reduces leakage of air from into the fuel reactor. The dried gases are analyzed for CO, CO_2, CH_4 (all IR sensors) and O_2 (paramagnetic sensors). The fuel-reactor flue gas is also analyzed in a gas chromatograph to verify these gas species and to further quantify N_2 and H_2.

2.1.2   10 kW Unit

The 10 kW laboratory-scale chemical-looping reactor system was constructed in 2002, and was used to perform the first successful demonstration of continuous chemical-looping combustion in 2003 [7]. A schematic of the unit is shown in Figure 4a.

1 – Air reactor (ID 150 mm)
  1.1 – Air-reactor fluidization (air)
2 – Riser (ID 80 mm, H_{tot} 2.2 m)
3 – Cyclone
  3.1 – Air-reactor gas outlet
4 – Upper loop seal
  4.1 – Loop-seal fluidization (nitrogen)
5 – Fuel reactor (ID 150 → 260 mm)
  5.1 – Fuel-reactor fluidization
        (fuel gas/nitrogen)
  5.2 – Fuel-reactor gas outlet
6 – Lower loop seal
  6.1 – Loop-seal fluidization (nitrogen)

(a) Schematic of the 10 kW chemical-looping combustion reactor

(b) 3D visualization of the fuel reactor (cut) with vertical separation wall between particle inlet and outlet

Figure 4: Illustrations of the 10 kW chemical-looping combustion reactor

The air reactor (ID 150 mm) tapers down to the riser (ID 80 mm), which drives the global circulation of solids. After the riser, gas and particles are separated in the cyclone. From the cyclone, particles fall down into a loop seal that prevents gas leakage between air reactor and fuel reactor. From the exit of the loop seal, particles flow into the bubbling bed of the fuel reactor. The fuel reactor is equipped with a vertical separation wall to prevent particles from bypassing the bed, see Figure 4b. Particles leave the fuel reactor through an overflow exit, which leads the particles, via the second loop-seal, back to the air reactor. Approximately 14-20 kg of oxygen-carrier particles are required to operate this unit.

The flue gases from air reactor and fuel reactor are first passively cooled through finned pipes before sample streams are withdrawn and led to a gas conditioning system. After the gas conditioning system, where the gas is cooled to 4°C and filtered, CO, CO_2, CH_4 and O_2 are measured continuously by infrared and paramagnetic sensors, respectively. An additional analysis of the fuel-reactor flue gas by a gas chromatograph is conducted to quantify N_2 and H_2. Not all particles are removed in the cyclone and, hence, the cyclone off-gas (= the air-reactor flue gas) is led to a bag filter, which captures elutriated particles and fines, before the filtered gas goes to the chimney. The fuel-reactor flue gas passes through a water seal, which has the dual purpose of collecting condensed steam and controlling the pressure in the fuel reactor.

2.2   Oxygen Carrier Materials

This work presents results of 14 calcium manganite-based materials that were tested in continuous chemical-looping operation. These materials represent only a fraction of all calcium manganite-based materials produced during development. Spherical particles in the size fraction of approximately 100-200 µm were produced by spray-drying with subsequent sintering. The reference materials were produced by the Flemish Institute for Technological Research NV (VITO) in Mol, Belgium, and the materials for raw-material substitution and upscaling were produced by Euro Support Advanced Materials B.V. in Uden, The Netherlands, cf. Table 1.

Before a material was considered adequate for testing in the 300 W unit, it had to show a sufficiently high reactivity in batch experiments, where only a few grams of oxygen carrier are tested and a sufficiently high resistance to mechanical attrition [8]. In order to be suitable for testing in the 10 kW unit, a material had to show low rates of attrition and degradation as well as a high conversion of fuel during continuous testing in the 300 W unit.

All oxygen carriers examined are based on calcium manganite with a perovskite structure, i.e., $CaMnO_{3-\delta}$, where δ expresses an oxygen deficiency. This type of material has so-called CLOU properties, i.e., it releases gas phase oxygen in the fuel reactor, which can react directly with the fuel [9]. This usually leads to an improved fuel conversion as compared to materials without CLOU properties [10].

Table 1 shows an overview of the different materials tested in the 300 W and 10 kW units. The addition of small amounts of Mg to the perovskite structure were found to improve fuel conversion, mechanical stability and fluidization properties [11]. Similarly, small amounts of Ti decrease the propensity of decomposition of the reactive phases [12].

Table 1: Overview of oxygen-carrier materials tested

	Oxygen-carrier notation	Sintering temp. (°C)	Conducted CLC tests 300 W	10 kW
[A]	C14-T (reference)	1300	☒	☒
	C28-TA (reference)	1300	☒	☒
[B]	C28-E1A	1350	☒	☐
	C28-C1A	1350	☒	☐
	C28-C2A	1350	☒	☐
	C28-E1S2	1335	☒	☒
	C28-E1S1	1335	☒	☐
	C28-C2S1	1335	☒	☐
[C]	C28-E3	1280[1]	☒	☐
	C28-E3	1320	☒	☐
	C28-E3	1280[2]	☒	☐
	C28-E5	1310	☒	☐
	C28-E5	1100	☒	☐
	C28-901	1100	☐	☒

[A] References (INNOCUOUS) **[B]** Raw-material substitution **[C]** Up-scaling
C14 … $CaMn_{0.9}Mg_{0.1}O_{3-\delta}$
C28 … $CaMn_{0.775}Mg_{0.1}Ti_{0.125}O_{3-\delta}$
-E3, -E5, -901 … Spray-drying batch numbers (same Mn and Ti sources as E1S2)
All other suffixes in oxygen-carrier notation refer to raw materials used, cf. Table 2

Table 2 shows an overview of the raw materials used for the production of the oxygen-carrier materials listed in Table 1. These raw materials represent only a fraction of all raw materials tested in the development process. In total, 13 different sources of manganese were used, which had a purity between 71% and > 99%. In addition, five different titanium sources were tested, which had a purity of 98.5% or more. In total, 24 different material compositions were produced and sintered at usually two different temperatures, which yielded 42 different batches produced.

Table 2: Sources of Mn and Ti used for the different oxygen-carrier materials

Notation (cf. Table 1)	Mn/Ti oxide	Purity (wt%)	Main impurity elements*	Raw material, supplier
T	Mn_3O_4	> 99	-	Trimanox, Chemalloy
E1	Mn_3O_4	96	Fe	Colormax P, Elkem
C1	MnO_2	81	Fe, Si, Al	CDMA (ground Mn ore), Erachem-Comilog
C2	Mn_3O_4	94	Fe, Si, Al, P	Hausmannite LM type, Erachem-Comilog
A	TiO_2 (rutile)	99.9	-	TiO_2 rutile, Alfa Aesar
S1	TiO_2 (rutile)	> 99	-	Sachtleben TR, Sachtleben
S2	TiO_2 (anatase)	> 99	-	Sachtleben M211, Sachtleben

* … all impurities are in oxide phase

2.3   Data Evaluation

The ability of an oxygen carrier to convert fuel to CO_2 is expressed by the CO_2 yield γ_{CO2}, see Equation (1), where $[i]_{FR}$ are the volume fractions of species i measured in the fuel reactor. The calculation is based on a carbon balance over the reactor system.

$$\gamma_{CO2} = \frac{[CO_2]_{FR}}{[CO_2]_{FR} + [CO]_{FR} + [CH_4]_{FR}} \tag{1}$$

3   RESULTS

3.1   Experiments in 300 W unit

3.1.1   CLOU properties

Figure 5 shows the release of gaseous oxygen in the fuel reactor under inert conditions at different temperatures. All materials show a considerable CLOU effect that increases with fuel-reactor temperature. The CLOU properties vary clearly for different raw materials and sintering temperatures used, see Figure 5a. During up-scaling, i.e., in Figure 5b, a clear correlation to the sintering temperature is not visible: The initial, unoptimized materials (C28-E3-1280[1]) and C28-E3-1320) show the lowest CLOU effect, followed by the material C28-E5-1100 and the material with highest sintering temperature (C28-E5-1310). The strongest CLOU effect is achieved by C28-E3-1280[2], which also had the lowest concentration of oxygen in the air reactor. It should be stressed that the combination of high amount of bed material in the fuel reactor and relatively low flow of inert gas, means that the concentration of oxygen at the outlet of the fuel reactor is likely limited by thermodynamics. Thus, these results say little about the rate of release. However, the results clearly show a strong oxygen uncoupling effect of all calcium manganite-based material produced.

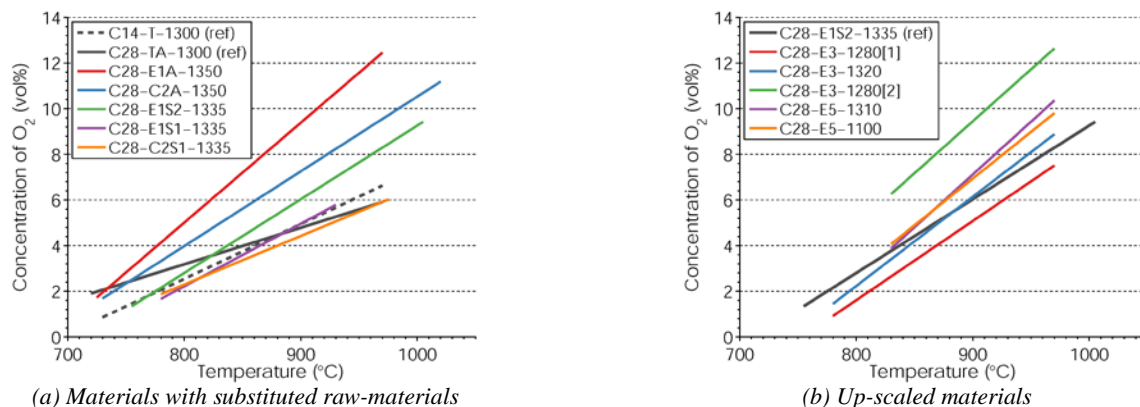|	
(a) Materials with substituted raw-materials	*(b) Up-scaled materials*

Figure 5: CLOU properties of calcium manganite-based materials during (a) raw material substitution and (b) up-scaling. Fitted lines are shown for the concentration of oxygen measured in the fuel reactor. The concentration of O_2 at the outlet of the air reactor was between 17.0 vol% and 19.6 vol%. No data was available for material C28-C1A-1350.

3.1.2   Fuel conversion

Figure 6 and Figure 7 show fuel conversion against specific fuel-reactor bed mass for the oxygen carriers produced with substituted raw-materials and up-scaled materials, respectively. The values shown are averages over periods of steady-state operation at 900°C and 950°C.
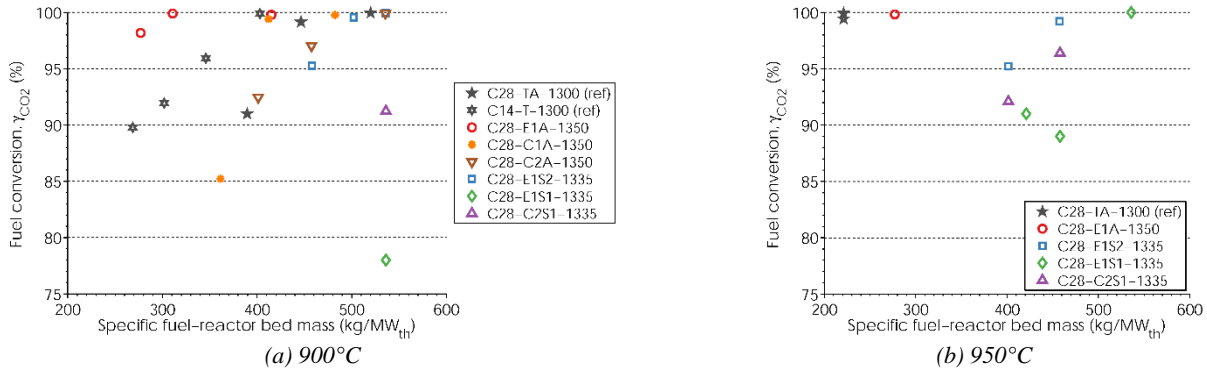

(a) 900°C   *(b) 950°C*

Figure 6: Fuel conversion, i.e., CO2 yield γ, as a function of the specific fuel-reactor bed mass at (a) 900°C and (b) 950°C for experiments performed in the 300 W unit. Data is shown for materials during raw-material substitution as well as reference materials C14-T and C28-TA, cf. Table 1.

All materials achieved very high levels of methane conversion, which was above 90% for most materials. An exception to this are the initial two up-scaled materials that were not optimized (C28-E3-1280[1] and C28-E3-1320). At 900°C, the performance of the material C28-E1S2-1335 came close to that of the reference oxygen-carrier from the INNOCUOUS project, C28-TA-1300, whereas at 950°C its performance was somewhat lower. During up-scaling, all materials, except the one that reacted with the saggars, were able to match the performance of C28-E1S2-1335, i.e., the reference material using low-cost raw materials.
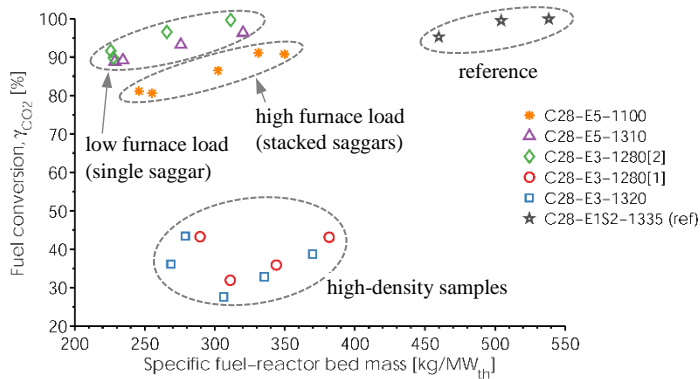

Figure 7: Fuel conversion, i.e., CO2 yield γCO2, at varied specific fuel-reactor bed mass at 900°C for experiments performed in the 300 W unit. Data is shown for materials during up-scaling as well as selected material C28-E1S2 from raw-material substitution, cf. Table 1.

3.1.3 Oxygen carrier properties

The density of the particles clearly increased with increasing sintering temperature. However, initial sinterings with stacked-saggar configuration (samples C28-E3-1320 and C28-E3-1280[1]), which is required for large-scale production, showed a higher density and a significantly lower fuel conversion in the 300 W tests, see Figure 8. Detailed investigations showed that in stacked saggars the reactivity of the material is increased, most probably due to a more reducing atmosphere. As a consequence, the sintering temperature had to be reduced significantly to achieve a similar density and reactivity. The materials C28-E5-1100 and C28-901-TR1100 sintered in stacked saggars show a similar density and reactivity as material sintered in open saggars at a temperature more than 200°C higher.
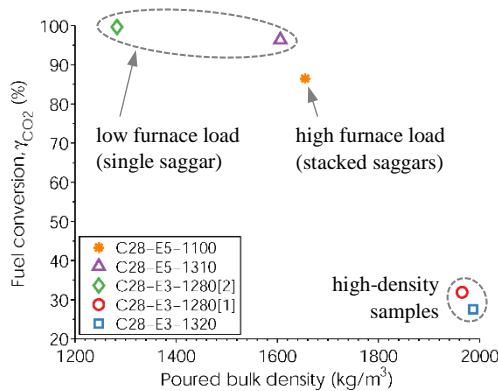

Figure 8: Oxygen carrier reactivity (here: fuel conversion γ_{CO2} at a temperature of 900°C and a specific fuel-reactor bed mass of 300-320 kg/MW$_{th}$) as a function of poured bulk density. Data is shown for materials during up-scaling.

3.2 Experiments in 10 kW unit

3.2.1 Fuel conversion

Figure 9 shows fuel conversion of different materials, i.e., SUCCESS materials C28-901, C28-E1S2 as well as reference materials C14-T and C28-TA (INNOCUOUS), at varied fuel input, i.e., specific fuel-reactor bed mass, and varied temperature. As is seen from the figure, the material C28-E1S2 was able to achieve comparable fuel conversion as the reference materials, produced in previous projects, i.e., C14-T and C28-TA. For the up-scaled material C28-901, the fuel conversion achieved was significantly lower, i.e., usually between 70% and 85%. It should be mentioned that the up-scaled material was operated for over 60 h at high temperature with a major leak upstream of the fuel reactor, which could have affected the oxygen carrier, although this is not known.
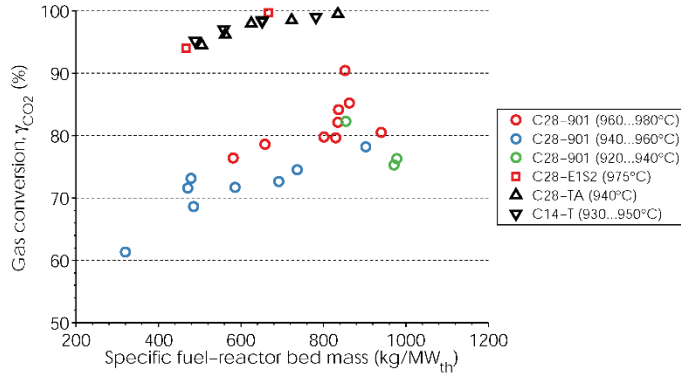
Figure 9: Fuel conversion, γ_{CO2}, at varied specific fuel-reactor bed mass for experiments performed in the 10 kW unit. Data is shown for the up-scaled material C28-901, the material selected during raw-material substitution (C28-E1S2) and the reference materials C14-T and C28-TA. The temperatures shown in the legend refer to fuel-reactor temperatures.

3.2.2 Particle attrition and Lifetime

The off-gas from the cyclone, i.e., Stream 3.1 in Figure 4a, is cooled and led through a bag filter, where particles and fines larger than 2 µm are captured. In parallel, the off-gas from the fuel reactor, i.e., Stream 5.2 in Figure 4a, is cooled and led through a water seal, where particles are retained. Due to the low gas velocities in the fuel reactor usually only fines are elutriated. The bag filter is emptied and its content sieved at least once per day, and the water seal is emptied and filtered about once per week.

For the materials tested here, fines production decreased significantly during the initial hours of fuel operation. The rate of fines production that followed this transition can was used to estimate a particle lifetime. Samples of the filter content in the fraction of 125-180 µm were analyzed in a customized jet-cup attrition test rig [15]. Values for estimated lifetimes based on operation in the 10 kW unit as well as attrition index, which is a measure for resistance against mechanical attrition, determined for fresh and used particles are shown in Table 3.

Table 3: Particle lifetime and attrition index for fresh and used particles based operation in 10 kW unit with data from [13, 14]

Oxygen carrier	Fuel operation (h)	Estimated lifetime (h)	Attrition index (wt%/h)	
			Fresh particles	Used particles
C14-T-1300	55	12 000	1.03	0.58
C28-TA-1300	99	9 000	8.86	1.93
C28-E1S2-1335	24	5 000	3.08	n/a
C28-901-1100	110	700	3.41	n/a

The fresh materials contained up to 4 wt% of particles below 90 µm, and, additionally, a fraction of irregular particles, e.g., micro agglomerates, hollow spheres and donut-shaped particles, which is common for a spray-drying process. These initial fines and irregular particles are likely the reason for the initially high rates of fines production. The attrition indices indicate that the average resistance to attrition increased during operation.

4   SUMMARY AND CONCLUSIONS

Calcium manganite-based oxygen carriers with a perovskite structure were developed for the application of chemical-looping combustion of gaseous, sulfur-free fuels. As part of two major EU-financed projects, a large number of materials have been produced using different raw materials and production parameters. These have been tested in a number of CLC pilot units, and the results of testing in two such reactors are described here. It is quite clear that the perovskite is simple to produce, also with highly heterogeneous and low-grade raw powders. The important CLOU property was seen for all oxygen carriers made. Several of the oxygen carrier produced with substituted raw-materials could match the performance of the reference materials produced with high-purity raw materials, and several oxygen carriers showed a combination of high reactivity and low attrition rates. Production was also scaled-up to multi-tonne scale. During up-scaling, the main challenges were related to the sintering process. Here, temperature gradients as well as inadequate gas exchange throughout large batches of material made the production of a material with homogeneous properties difficult. This issue is likely to be relatively easy solved by using rotary kilns instead of chamber furnaces for the sintering process.

5   ACKNOWLEDGEMENT

REFERENCES

[1]   Lyngfelt A., Leckner B. and Mattisson T. *A fluidized-bed combustion process with inherent CO$_2$ separation; application of chemical-looping combustion*. Chemical Engineering Science: 56, pp.3101-3113, 2001.

[2]   Adánez J., Abad A., García-Labiano F., Gayán P. and de Diego L.F. *Progress in chemical-looping combustion and reforming technologies*. Progress in Energy and Combustion Science: 38, pp.215-282, 2012.

[3]   Mattisson T., Adánez J., Mayer K., Snijkers F., Williams G., Wesker E., Bertsch O. and Lyngfelt A. *Innovative Oxygen Carriers Uplifting Chemical-looping Combustion*. Energy Procedia: 63, pp.113-130, 2014.

[4]   Imtiaz Q., Hosseini D. and Müller C.R. *Review of Oxygen Carriers for Chemical Looping with Oxygen Uncoupling (CLOU): Thermodynamics, Material Development, and Synthesis*. Energy Technology: 1, pp.633-647, 2013.

[5]   Lyngfelt A., Kronberger B., Adanez J., Morin J.X. and Hurst P. *The GRACE project: Development of oxygen carrier particles for chemical-looping combustion. Design and operation of a 10 kW chemical-looping combustor*. Greenhouse Gas Control Technologies: I, pp.115-123, 2005.

[6]   Mattisson T., Adanez J., Proell T., Kuusik R., Beal C., Assink J., Snijkers F. and Lyngfelt A. *Chemical-looping Combustion CO₂ Ready Gas Power*. Energy Procedia: 1, pp.1557-1564, 2009.

[7]   Lyngfelt A. and Thunman H., *Construction and 100 h of operational experience of a 10-kW chemical looping combustor*, in *Carbon Dioxide Capture for Storage in Deep Geologic Formations - Results from the CO₂ Capture Project*, DC Thomas and SM Benson, Editors. 2005, Elsevier Science Ltd: London. p. 625-646.

[8]   Jing D., Jacobs M., Hallberg P., Lyngfelt A. and Mattisson T. *Development of $CaMn_{0.775}Mg_{0.1}Ti_{0.125}O_{3-\delta}$ oxygen carriers produced from different Mn and Ti sources*. Materials and Design: 89, pp.527-542, 2016.

[9]   Rydén M., Lyngfelt A. and Mattisson T. *$CaMn_{0.875}Ti_{0.125}O_3$ as oxygen carrier for chemical-looping combustion with oxygen uncoupling (CLOU)—Experiments in a continuously operating fluidized-bed reactor system*. International Journal of Greenhouse Gas Control: 5, pp.356-366, 2011.

[10]   Moldenhauer P., Rydén M., Mattisson T. and Lyngfelt A. *Chemical-looping combustion and chemical-looping with oxygen uncoupling of kerosene with Mn- and Cu-based oxygen carriers in a circulating fluidized-bed 300W laboratory reactor*. Fuel Processing Technology: 104, pp.378-389, 2012.

[11]   Hallberg P., Jing D., Rydén M., Mattisson T. and Lyngfelt A. *Chemical looping combustion and chemical looping with oxygen uncoupling experiments in a batch reactor using spray-dried $CaMn_{1-x}M_xO_{3-\delta}$ (M = Ti, Fe, Mg) particles as oxygen carriers*. Energy and Fuels: 27, pp.1473-1481, 2013.

[12]   Leion H., Larring Y., Bakken E., Bredesen R., Mattisson T. and Lyngfelt A. *Use of $CaMn_{0.875}Ti_{0.125}O_3$ as oxygen carrier in chemical-looping with oxygen uncoupling*. Energy and Fuels: 23, pp.5276-5283, 2009.

[13]   Källén M., Rydén M., Dueso C., Mattisson T. and Lyngfelt A. *$CaMn_{0.9}Mg_{0.1}O_{3-\delta}$ as oxygen carrier in a gas fired 10 kW_{th} chemical-looping combustion unit*. Industrial & Engineering Chemistry Research: 52, pp.6923-6932, 2013.

[14]   Hallberg P., Hanning M., Rydén M., Mattisson T. and Lyngfelt A. *Investigation of a calcium manganite as oxygen carrier during 99 h of operation of chemical-looping combustion in a 10 kW_{th} reactor unit*. International Journal of Greenhouse Gas Control: 53, pp.222-229, 2016.

[15]   Rydén M., Moldenhauer P., Lindqvist S., Mattisson T. and Lyngfelt A. *Measuring attrition resistance of oxygen carrier particles for chemical looping combustion with a customized jet cup*. Powder Technology: 256, pp.75-86, 2014.